

Crystallization kinetics and morphology of poly(ethylene suberate)

Shoutian Qiu, Zhaobin Qiu

State Key Laboratory of Chemical Resource Engineering, MOE Key Laboratory of Carbon Fiber and Functional Polymers, Beijing University of Chemical Technology, Beijing 100029, China
Correspondence to: Z. Qiu (E-mail: qiuzb@mail.buct.edu.cn)

ABSTRACT: The crystallization kinetics and morphology of poly(ethylene suberate) (PESub) were studied in detail with differential scanning calorimetry, polarized optical microscopy, and wide-angle X-ray diffraction. The Avrami equation could describe the overall isothermal melt crystallization kinetics of PESub at different crystallization temperatures; moreover, the overall crystallization rate of PESub decreased with increasing crystallization temperature. The equilibrium melting point of PESub was determined to be 70.8°C. Ring-banded spherulites and a crystallization regime II to III transition were found for PESub. The Tobin equation could describe the nonisothermal melt crystallization kinetics of PESub at different cooling rates, while the Ozawa equation failed. © 2015 Wiley Periodicals, Inc. *J. Appl. Polym. Sci.* **2016**, *133*, 43086.

KEYWORDS: crystallization; morphology; polyesters

Received 28 August 2015; accepted 25 October 2015

DOI: 10.1002/app.43086

INTRODUCTION

Recently, more and more attention has been paid to the development and research of some aliphatic polyesters because they are promising biodegradable materials, due to their green, environmentally friendly, and biodegradable nature.¹ Aliphatic polyesters are usually susceptible to hydrolytic or enzymatic degradation in natural environments and also have physical properties comparable to many traditional thermoplastics.² Among all the aliphatic polyesters, poly(ethylene succinate) (PES) and poly(butylene succinate) (PBS) are two typical ones, which not only have attracted considerable attention and interest but also have been commercially available. Therefore, the crystallization behavior, spherulitic morphology, spherulitic growth kinetics, and melting behavior of PES and PBS have been extensively investigated and reported in literature.^{3–15}

Poly(ethylene suberate) (PESub) is also an aliphatic polyester, and it can be derived from ethylene glycol and suberic acid via a melt polycondensation method.¹⁶ It has a chemical structure similar to that of PES but possesses more methylene units than PES. Unlike the extensively investigated PES,^{5–8,13,17–29} only a few works have focused on PESub.^{30–36} Turner-Jones and Bunn studied the crystal structure of PESub in 1962 and determined it to be a monoclinic unit cell with dimensions of $a = 5.51$ Å, $b = 7.25$ Å, c (fiber axis) = 14.28 Å, and $\beta = 114.30^\circ$.³⁰ Similar results were also reported by other researchers.^{31–34} Bradbury *et al.* studied the spectrum of oriented films of PESub with polarized infrared fraction and found striking differences in the spectrum between the amorphous and crystalline regions.³⁵

Ueberreiter *et al.* studied and determined heat of fusion, melting temperature, degrees of crystallization, and entropies of fusion of PESub.³⁶ Keith *et al.* once observed unexpected morphological changes in PESub upon blending with small concentrations (1%) of poly(vinyl butyral) (PVB) and found that the blending with a small amount of PVB greatly decreased the nucleation density of PESub spherulites.¹⁶

It is well known that the crystallization process greatly affects the crystalline structure, morphology, mechanical and physical properties, and degradation of aliphatic polymers.^{3,37–40} To the best of our knowledge, the crystallization kinetics and morphology of PESub have not been reported in detail in the literature until now. Therefore, we investigated the crystallization kinetics and morphology of PESub in detail with several techniques under different crystallization conditions. This may be of great importance and help for a better understanding of the crystallization kinetics and morphology and a wider application of PESub from both academic and practical viewpoints.

EXPERIMENTAL

PESub ($M_n = 2.6 \times 10^4$ g/mol, $M_w = 8.2 \times 10^4$ g/mol) was synthesized in our laboratory via a two-step melt polycondensation method.⁴¹

A TA Instruments differential scanning calorimeter (DSC) Q100 (New Castle, Delaware) was used for the thermal analysis of PESub under different crystallization conditions. All samples were first annealed at 100°C for 3 min to erase any previous thermal history before the following process. For the isothermal

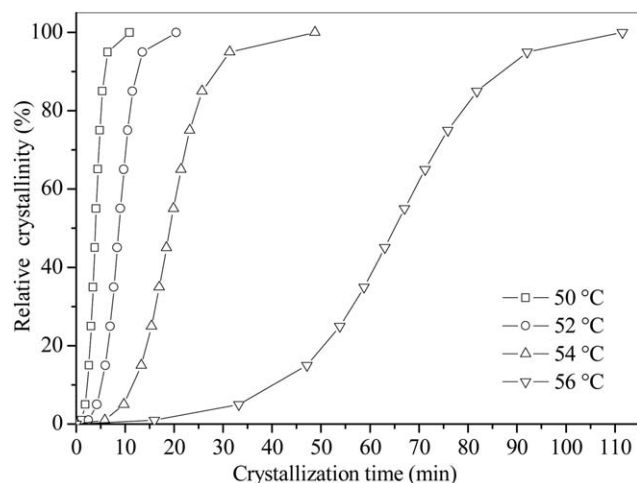


Figure 1. Plots of relative crystallinity versus crystallization time of PESub.

crystallization process, the samples were quenched to the predetermined crystallization temperature (T_c) as fast as possible, crystallized for a period of time, and heated to 100°C at 10°C/min. For the nonisothermal crystallization process, the samples were cooled to -80°C at various cooling rates and then heated to 100°C at 10°C/min.

The spherulitic morphology and growth rate of PESub were studied by a polarized optical microscope (POM) (Olympus BX51) (Tokyo, Japan) equipped with a temperature controller (Linkam THMS 600) (Surrey, England). The spherulitic growth rate (G) was obtained from the variation of radius (R) with time (t): $G = dR/dt$.

The wide-angle X-ray diffraction pattern (WAXD) of PESub was recorded on a Rigaku D/Max 2500 VB2t/PC (Tokyo, Japan) X-ray diffractometer at a speed of 4°/min from 5° to 50°. The WAXD was operated at 40 kV and 200 mA at room temperature.

RESULTS AND DISCUSSION

Isothermal Melt Crystallization Kinetics of PESub

The overall isothermal melt crystallization kinetics of PESub was first performed with DSC in a wide range of T_c . Figure 1 demonstrates the development of relative crystallinity with crystallization time for PESub at different T_c values from 48 to 56°C. From Figure 1, with the increase of T_c , the required crystallization time of PESub was prolonged, suggesting that the crystallization process was retarded at higher T_c .

The overall isothermal melt-crystallization kinetics of PESub was analyzed by the Avrami equation. The relative crystallinity (X_t) develops with crystallization time (t) as follows:

$$1 - X_t = \exp(-kt^n) \quad (1)$$

where n is the Avrami exponent, which depends on the nature of nucleation and growth geometry of the crystals, and k is the crystallization rate constant involving both nucleation and growth rate parameters.⁴²

As illustrated in Figure 2, the Avrami plots of PESub displayed almost parallel straight lines, indicating that the Avrami method could describe the overall isothermal melt-crystallization

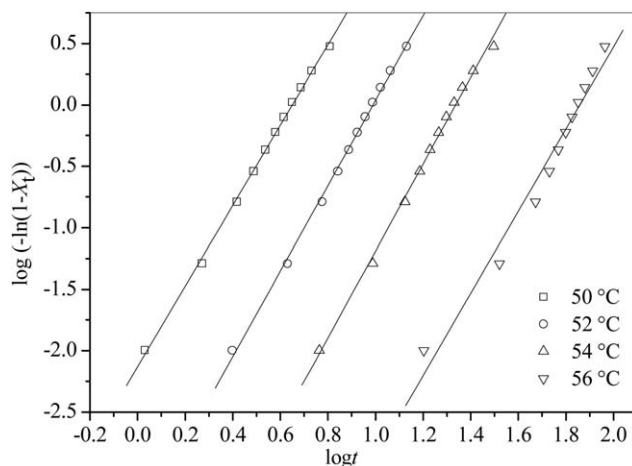


Figure 2. Avrami plots of PESub at indicated T_c values.

processes. The n and k values were obtained from the Avrami plots. For comparison, Table I lists all of the related parameters. The n values slightly varied between 3.1 and 3.5; moreover, they were not remarkably affected by T_c , indicating that the crystallization mechanism of PESub did not change in the investigated T_c range and may correspond to a three-dimensional truncated growth with thermal nucleation.⁴³

Crystallization half-time ($t_{0.5}$), the time required to achieve 50% of the final crystallinity, was used for discussing the crystallization kinetics of PESub. The $t_{0.5}$ values were calculated according to the Avrami equation:

$$t_{0.5} = \left(\frac{\ln 2}{k} \right)^{1/n} \quad (2)$$

Table I includes the $t_{0.5}$ values. From Table I, the $t_{0.5}$ values increased with an increase in T_c , indicative of a slower crystallization rate at higher T_c . Accordingly, the reciprocal values of $t_{0.5}$ ($1/t_{0.5}$) were used to compare the overall isothermal melt crystallization rate. From Table I, $1/t_{0.5}$ decreased with the increase of T_c , suggesting a slower overall isothermal crystallization rate at higher T_c because of a smaller degree of supercooling. In brief, the increase of T_c did not modify the crystallization mechanism but apparently reduced the overall isothermal melt-crystallization rate of PESub.

Figure 3 illustrates the subsequent melting behavior of PESub after crystallizing at the indicated T_c values. Despite T_c , PESub only presented one melting endotherm; moreover, with increasing T_c , the melting endotherm moved gradually to higher temperature.

Table I. Isothermal Crystallization Kinetics Parameters of PESub

T_c (°C)	n	K (min ⁻ⁿ)	$t_{0.5}$ (min)	$1/t_{0.5}$ (min ⁻¹)
50	3.3	7.4×10^{-3}	4.0	2.5×10^{-1}
52	3.5	3.7×10^{-4}	8.8	1.1×10^{-1}
54	3.5	1.9×10^{-5}	19.6	5.1×10^{-2}
56	3.3	6.1×10^{-7}	64.7	1.5×10^{-2}

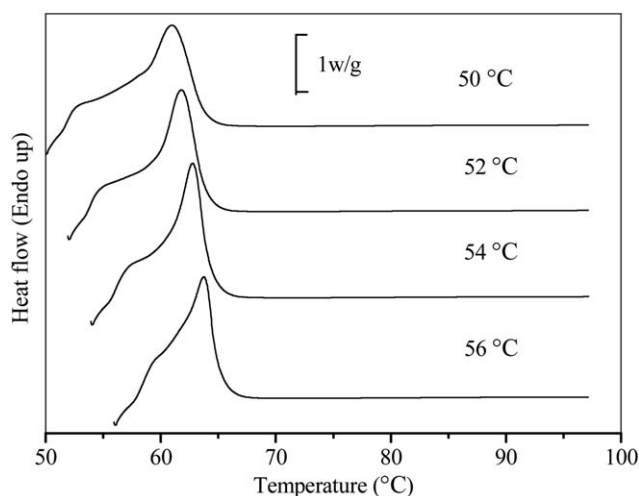


Figure 3. Melting behavior of PESub after isothermally crystallizing at indicated T_c values.

The equilibrium melting point (T_m^o) is an important parameter of semicrystalline polymers, and it may be derived from the Hoffmann–Weeks equation:

$$T_m = \eta T_c + (1 - \eta) T_m^o \quad (3)$$

where T_m corresponds to the apparent melting point at T_c and η may be regarded as a measure of the stability.⁴⁴ On the basis of the results shown in Figure 3, Figure 4 shows the Hoffman–Weeks plot for PESub. From Figure 4, T_m^o was calculated to be as 70.8°C, and the η value was determined to be 0.45.

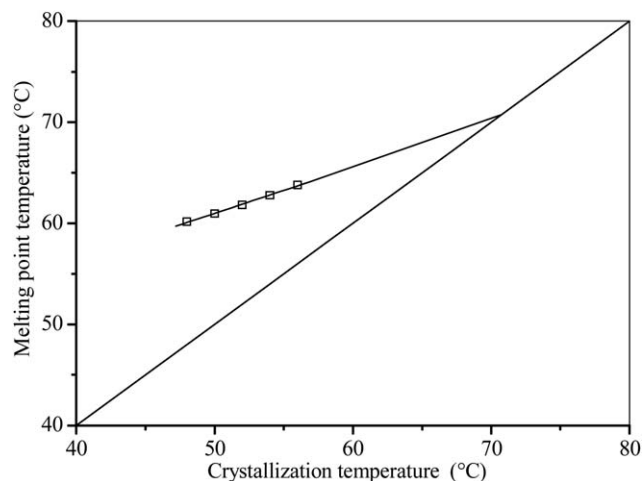


Figure 4. Hoffman–Weeks plot of PESub.

Spherulitic Morphology, Regime Transition, and Crystal Structure of PESub

It is important to investigate the spherulitic morphology and growth rate of PESub because they may affect its final physical properties. In this section, the spherulitic morphology and growth rate of PESub were studied with POM in a wide range of T_c . Figure 5 displays the POM images of PESub after completely crystallizing at 50, 52, 54, and 56°C. From Figure 5, PESub presented ring-banded spherulites at all investigated T_c values. The formation of ring-banded spherulites was probably attributed to the cooperative lamellar twisting in the direction of radial growth.⁴⁵

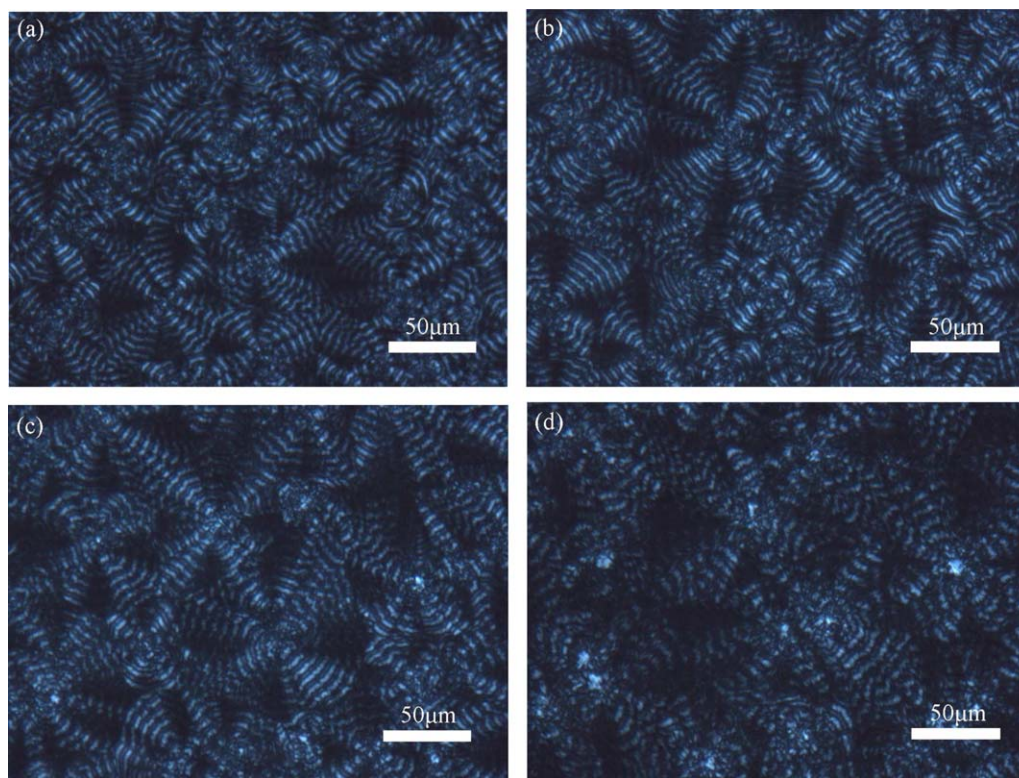


Figure 5. POM images of PESub crystallized at (a) 50, (b) 52, (c) 54, and (d) 56°C. [Color figure can be viewed in the online issue, which is available at wileyonlinelibrary.com.]

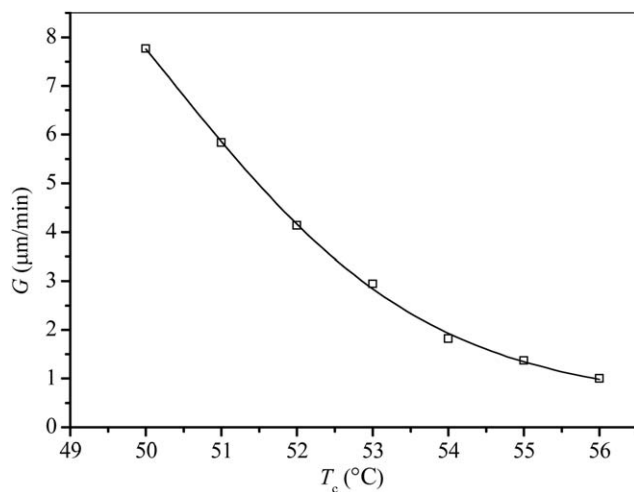


Figure 6. Temperature dependence of spherulitic growth rates of PESub.

Figure 6 summarizes the measured spherulitic growth rates of PESub in a wide range of T_c . For instance, at a T_c of 50°C, PESub showed a G value of 7.8 $\mu\text{m}/\text{min}$, whereas it displayed a G value of 1.0 $\mu\text{m}/\text{min}$ at 56°C. It was clear that the G values decreased with the increase of T_c . Such reduction of G with increasing T_c is very common in polymer crystallization.

To further study the spherulitic growth kinetics of PESub, the secondary nucleation theory, that is, the Lauritzen–Hoffman equation, was used to analyze the spherulitic growth rate of PESub. On the basis of the secondary nucleation theory, the spherulitic growth rate can be described as

$$G = G_0 \exp\left[-\frac{U^*}{R(T_c - T_\infty)}\right] \exp\left[-\frac{K_g}{T_c(\Delta T)f}\right] \quad (4)$$

where G_0 is a pre-exponential factor, U^* is the activation energy for transporting the polymer chain segments to the crystallization site, R is the gas constant, T_∞ is a temperature below which the polymer chain movement ceases, ΔT is the degree of supercooling described as $T_m^0 - T_c$, f is a correction factor accounting for the variation in the enthalpy of fusion given as $f = 2T_c/(T_m^0 + T_c)$, and K_g is the nucleation constant, given as follows:

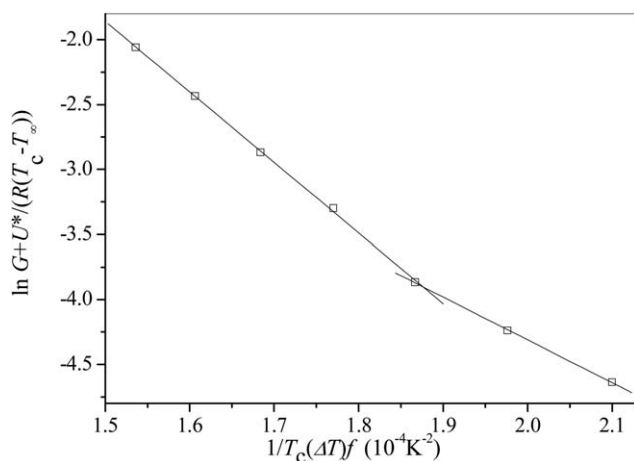


Figure 7. Crystallization-regime transition analysis of PESub.

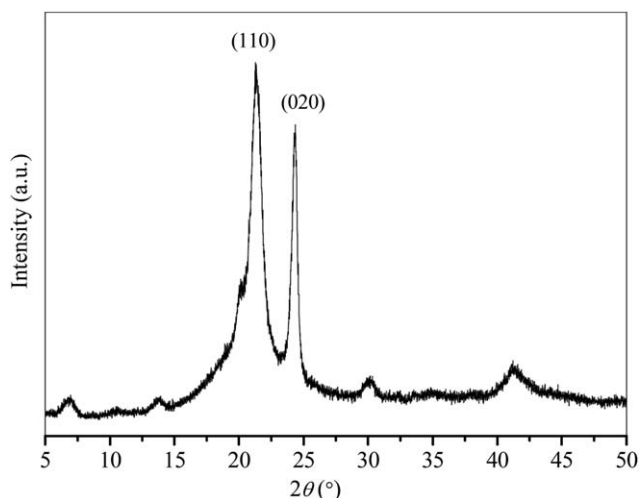


Figure 8. WAXD pattern of PESub crystallized at 56°C.

$$K_g = \frac{mb_0\sigma\sigma_e T_m^0}{\Delta h_f k} \quad (5)$$

where σ and σ_e are the lateral-surface free energy and end-surface free energy, respectively; b_0 is the molecular thickness; Δh_f is the heat of fusion per unit volume; k is the Boltzmann constant; and m is a constant dependent on the crystallization regime, which is equal to 4 in regime I and III but 2 in regime II.^{46,47} According to the Williams–Landel–Ferry equation, the values of $U^* = 17,246.3$ J/mol and $T_\infty = T_g - 51.6$ K were used in this work.⁴⁸

Figure 7 displays the Lauritzen–Hoffman plot for PESub. As seen from Figure 7, the experimental data were fitted well by two straight lines with different slopes, indicating that there were two crystallization regimes. On the basis of the Lauritzen–Hoffman theory, such discontinuity should be attributed to a transition from regime II to regime III. The regime transition temperature (T_{tr}) between regimes II and III was obtained from the intersection point of the two straight lines shown in Figure 7; moreover, the values of K_{gIII} and K_{gII} , corresponding to the K_g values in regime III and II, were determined to be 5.43 \times

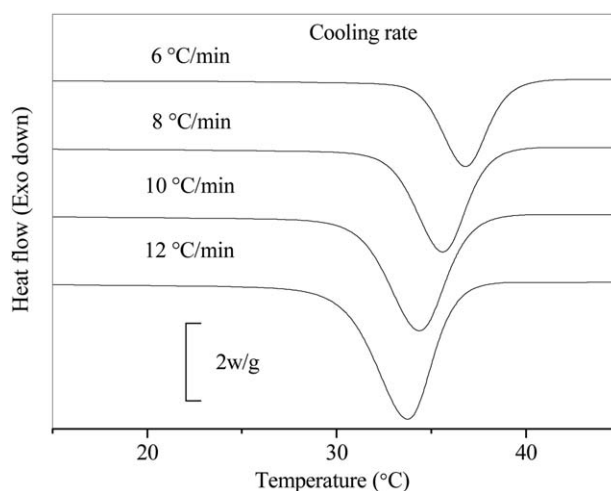


Figure 9. Nonisothermal melt-crystallization behavior of PESub crystallized at various cooling rates.

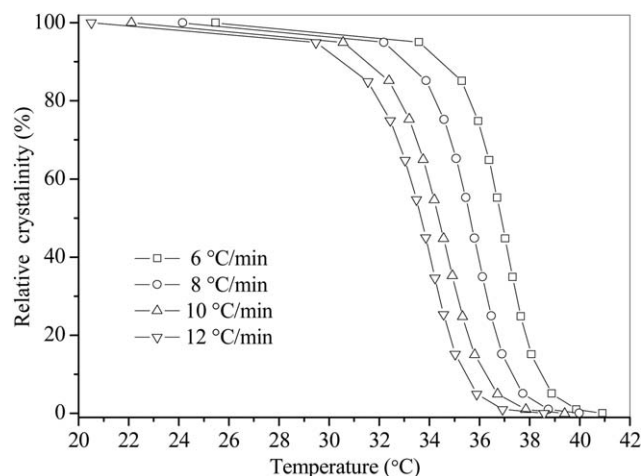


Figure 10. Plots of relative crystallinity versus crystallization temperature.

10^5 and $3.31 \times 10^5 \text{ K}^2$, respectively, from Figure 7. The K_{gIII}/K_{gII} value was estimated to be around 1.6 for PESub, which was slightly less than 2 according to the theory. The T_{tr} of PESub was around 54°C .

Figure 8 illustrates the WAXD pattern of PESub, which was completely crystallized at 56°C . As shown in Figure 8, PESub was characterized by the two strong diffraction peaks at 21.5° and 24.2° , corresponding to the (110) and (020) planes, respectively.³⁰ Based on the WAXD pattern, the degree of crystallinity value of PESub was estimated to be around 55%, which was calculated by the ratio of the area under the crystalline peaks to the whole area under both the crystalline peaks and the amorphous peaks background, indicating that PESub was a highly crystalline polymer.

Nonisothermal Melt Crystallization Kinetics of PESub

The nonisothermal crystallization behavior of PESub was further investigated with DSC. Figure 9 illustrates the DSC traces of PESub crystallized nonisothermally from the crystal-free melt at a series of cooling rates of 6, 8, 10, and $12^\circ\text{C}/\text{min}$. With the increase of cooling rate, the well-defined crystallization exotherms shifted to the lower-temperature region, indicating that the crystallization of PESub was retarded.

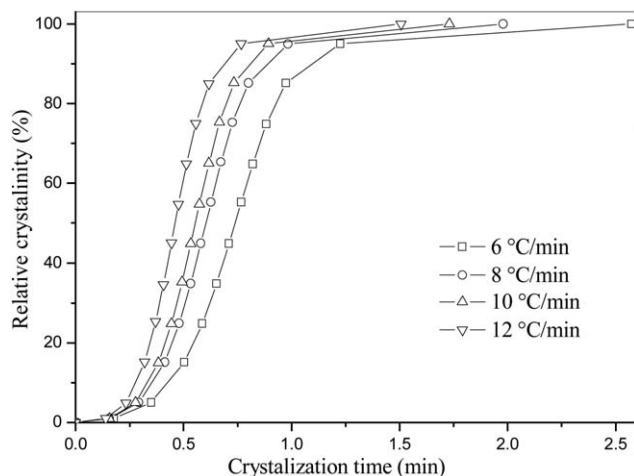


Figure 11. Plots of relative crystallinity versus crystallization time.

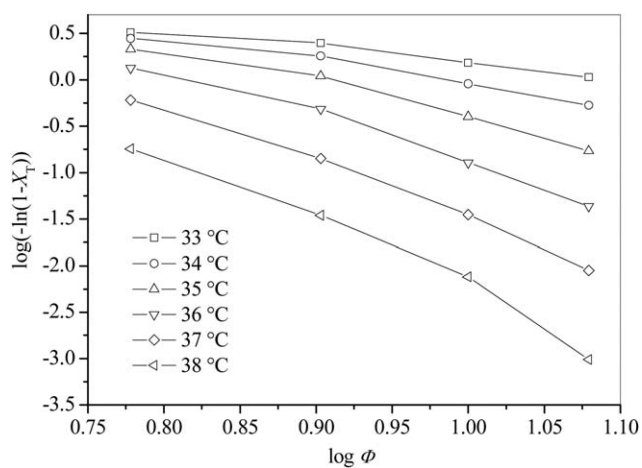


Figure 12. Ozawa plots of PESub at different cooling rates.

It was of great interest to study the effect of cooling rate on the variation of crystallization peak temperature (T_p) of PESub. From Figure 9, a crystallization peak temperature (T_p) of about 36.8°C was found for PESub at $6^\circ\text{C}/\text{min}$; however, the T_p values decreased to 35.6, 34.5, and 33.8°C with increasing cooling rate to 8, 10, and $12^\circ\text{C}/\text{min}$, respectively. In addition, the nonisothermal melt-crystallization enthalpy values were measured to be 70.3, 72.9, 71.6, and 70.1 J/g when PESub was crystallized at 6, 8, 10, and $12^\circ\text{C}/\text{min}$, respectively. Within the investigated cooling rates, the crystallization enthalpy values varied slightly, suggesting that the cooling rate slightly affected the crystallinity value during the nonisothermal melt crystallization process.

Figure 10 shows the plots of relative crystallinity versus crystallization temperature of PESub. During the nonisothermal melt-crystallization process, the relationship between crystallization time (t) and crystallization temperature (T) could be described as

$$t = \frac{T_0 - T}{\Phi} \quad (6)$$

where Φ is the cooling rate and T_0 is the onset temperature of crystallization. Therefore, the plots of relative crystallinity as a function of crystallization temperature shown in Figure 10 could thus be transformed into the plots of relative crystallinity

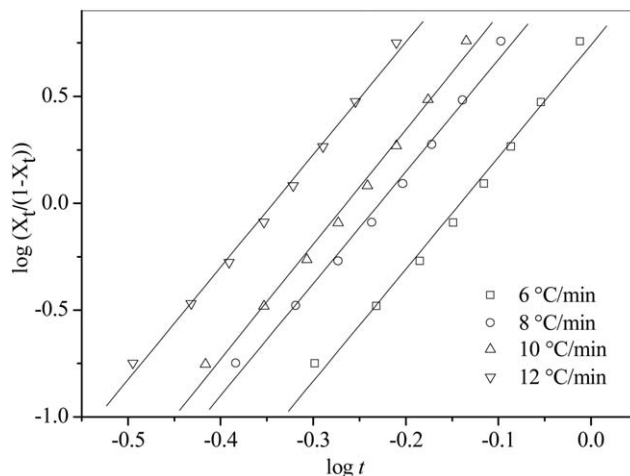


Figure 13. Tobin plots of PESub at different cooling rates.

Table II. Nonisothermal Crystallization Kinetics Parameters of PESub Obtained from the Tobin Method

Φ (°C/min)	n_t	k_t (min ⁻ⁿ)	T_p (°C)
6	5.3	5.5	36.8
8	5.2	15.7	35.6
10	5.4	24.1	34.5
12	5.3	64.0	33.8

as a function of crystallization time (Figure 11). Figure 11 shows the plots of relative crystallinity as a function of crystallization time for PESub. It was obvious that with the increase of the cooling rate, the crystallization time became shorter.

In the present work, two methods, the Ozawa method and the Tobin method, were employed to investigate the nonisothermal crystallization kinetics of PESub.^{49–52} The Ozawa equation is described as follows:

$$X_T = 1 - \exp\left(\frac{-K(T)}{\Phi^m}\right) \quad (7)$$

where X_T is the relative crystallinity, $K(T)$ is the cooling (or heating) function at crystallization temperature T , and m is the Ozawa exponent that depends on the type of nucleation and growth mechanism.⁴⁹ Figure 12 shows the Ozawa plots of PESub at the indicated T_c values. According to the equation, obvious linear plots should be found if it can describe the nonisothermal crystallization behavior of PESub; however, linear lines were not observed, indicating an inapplicability of the Ozawa equation in analyzing the nonisothermal crystallization kinetics. The failure of the application of the Ozawa method to the nonisothermal crystallization process of PESub may be related to the occurrence of the secondary crystallization. Similar phenomena were also found in PBS and poly(aryl ether ketones) (PAEKs).^{13,53}

The nonisothermal crystallization kinetics of PESub were further studied by the Tobin method, which suggested a theory of phase transformation kinetics with growth-site impingement to describe the nonisothermal crystallization process of polymers.^{50–52} According to this approach, the equation of phase transition is described as follows:

$$X_t = \frac{k_t t^{n_t}}{1 + k_t t^{n_t}} \quad (8)$$

where X_t is the relative crystallinity as a function of time, k_t is the Tobin crystallization rate constant, and n_t is the Tobin exponent.^{50–52}

Figure 13 shows the Tobin plots for PESub, from which the n_t and k_t values were obtained, as listed in Table II. The values of n_t varied between 4.0 and 4.4. In contrast, the values of k_t increased with the increase in the cooling rate. The values of k_t at a faster cooling rate are larger than those at a slower cooling rate, indicating that the crystallization of PESub was retarded with the decrease in the cooling rate.

CONCLUSIONS

The overall isothermal melt-crystallization kinetics, spherulitic morphology and growth, crystallization regime transition, and

nonisothermal melt-crystallization kinetics of PESub were studied in detail with DSC, POM, and WAXD in this work. The Avrami equation can describe the isothermal melt-crystallization kinetics of PESub; meanwhile, the n values of PESub slightly varied between 3.1 and 3.5 and were not remarkably affected by crystallization temperature. The equilibrium melting point of PESub was determined to be 70.8°C. The WAXD result indicated that PESub is a highly semicrystalline polymer. The spherulitic morphology of PESub was observed with POM, and ring-banded spherulites were formed in the investigated crystallization temperature range. On the basis of the Lauritzen–Hoffman theory, PESub exhibited a crystallization regime II to III transition; furthermore, the regime transition temperature was around 54°C. The nonisothermal melt crystallization kinetics of PESub was studied by DSC at various cooling rates. The Ozawa equation failed to describe the nonisothermal melt crystallization kinetics of PESub. The Tobin method could fit the nonisothermal melt crystallization process very well, and the related crystallization kinetics parameters were obtained.

ACKNOWLEDGMENTS

Part of this work was supported by the National Natural Science Foundation, China (51573016, 51373020, and 51221002).

REFERENCES

- Wang, T.; Wang, T.; Li, H.; Gan, Z.; Yan, S. *Phys. Chem. Chem. Phys.* **2009**, *11*, 1619.
- Noguchi, K.; Kondo, H.; Ichikawa, Y.; Okuyama, K.; Washiyama, J. *Polymer* **2005**, *46*, 10823.
- Lu, X.; Hay, J. *Polymer* **2001**, *42*, 9423.
- Rybníkář, F. *J. Polym. Sci.* **1960**, *44*, 517.
- Gan, Z.; Abe, H.; Doi, Y. *Biomacromolecules* **2000**, *1*, 704.
- Gan, Z.; Abe, H.; Doi, Y. *Biomacromolecules* **2000**, *1*, 713.
- Qiu, Z.; Ikehara, T.; Nishi, T. *Polymer* **2003**, *44*, 5429.
- Qiu, Z.; Komura, M.; Ikehara, M.; Nishi, T. *Polymer* **2003**, *44*, 7781.
- Ihn, K.; Yoo, E.; Im, S. *Macromolecules* **1995**, *28*, 2460.
- Ichikawa, Y.; Suzuki, J.; Washiyama, J.; Moteki, Y.; Noguchi, K.; Okuyama, K. *Polymer* **1994**, *35*, 3338.
- Yoo, E.; Im, S. *J. Polym. Sci. Polym. Phys.* **1999**, *37*, 1357.
- Miyata, T.; Masuko, T. *Polymer* **1998**, *39*, 1399.
- Qiu, Z.; Fujinami, S.; Komura, M.; Nakajima, K.; Ikehara, T.; Nishi, T. *Polym. J.* **2004**, *36*, 642.
- Papageorgiou, G.; Achilias, D.; Bikiaris, D. *Macromol. Chem. Phys.* **2007**, *208*, 1250.
- Qiu, Z.; Yang, W. *J. Appl. Polym. Sci.* **2007**, *104*, 972.
- Keith, H. D.; Padden, Jr., F. J. *Macromolecules* **1989**, *22*, 666.
- Qiu, Z.; Fujinami, S.; Komura, M.; Nakajima, K.; Ikehara, T.; Nishi, T. *Polymer* **2004**, *45*, 4515.
- Lu, J.; Qiu, Z.; Yang, W. *Polymer* **2007**, *48*, 4196.
- Miao, L.; Qiu, Z.; Yang, W.; Ikehara, T. *React. Funct. Polym.* **2008**, *68*, 446.
- Zhu, S.; Zhao, Y.; Qiu, Z. *Thermochim. Acta* **2011**, *517*, 74.

21. Yang, Y.; Qiu, Z. *J. Appl. Polym. Sci.* **2011**, *122*, 105.
22. Wu, H.; Qiu, Z. *CrystEngComm* **2012**, *14*, 3586.
23. Qiu, Z.; Ikehara, T.; Nishi, T. *Macromolecules* **2002**, *35*, 8251.
24. Lu, J.; Qiu, Z.; Yang, W. *Macromolecules* **2008**, *41*, 141.
25. Tang, L.; Qiu, Z. *Ind. Eng. Chem. Res.* **2014**, *53*, 11365.
26. Ikehara, T.; Ito, D.; Kataoka, T. *Polym. J.* **2015**, *47*, 379.
27. Jing, X.; Qiu, Z. *Ind. Eng. Chem. Res.* **2014**, *53*, 498.
28. Wu, F.; Huang, C.; Zeng, J.; Li, S.; Wang, W. *RSC Adv.* **2014**, *4*, 54175.
29. Zhao, Z.; Wang, X.; Zhou, W.; Zhi, E.; Zhang, W.; Ji, J. *J. Appl. Polym. Sci.* **2013**, *130*, 3212.
30. Turner-Jones, A.; Bunn, W. *Acta. Cryst.* **1962**, *15*, 105.
31. Hobbs, S.; Billmeyer, F. J. *Polym. Sci. Polym. Phys.* **1969**, *7*, 1119.
32. Fuller, C. S.; Frosch, C. J. *J. Phys. Chem.* **1939**, *43*, 323.
33. Liao, W. B.; Boyd, R. H. *Macromolecules* **1990**, *23*, 1531.
34. Fuller, C. S.; Baker, W. O. *J. Chem. Educ.* **1943**, *20*, 3.
35. Bradbury, E. M.; Elliott, A.; Fraser, R. D. B. *Trans. Faraday Soc.* **1960**, *56*, 1117.
36. Ueberreiter, K.; Karl, V.-H.; Altmeyer, A. *Eur. Polym. J.* **1978**, *14*, 1045.
37. Im, S.; Kim, T.; Han, S.; Moon, T.; Bae, Y. *J. Appl. Polym. Sci.* **1997**, *65*, 1745.
38. Zhang, F.; Zhou, L.; Xiong, Y.; Xu, W. *J. Polym. Sci. Polym. Phys.* **2008**, *46*, 2201.
39. Supaphol, P. *Thermochim. Acta* **2001**, *370*, 37. <http://www.science-direct.com/science/article/pii/S004060310000767X> - CORR1
40. Pan, B.; Yue, Q.; Ren, J.; Wang, H.; Jian, L.; Zhang, J.; Yang, S. *J. Macromol. Sci. Phys.* **2006**, *45*, 1025.
41. Yang, Y.; Qiu, Z. *CrystEngComm* **2011**, *13*, 2408.
42. Avrami, M. *J. Chem. Phys.* **1940**, *8*, 212.
43. Wunderlich, B. *Macromolecular Physics, Crystal Nucleation, Growth, Annealing*; Academic Press: New York, **1976**; Vol. 2.
44. Hoffman, J.; Weeks, J. *J. Chem. Phys.* **1965**, *42*, 4301.
45. Woo, E.; Wu, P.; Wu, M.; Yan, K. *Macromol. Chem. Phys.* **2006**, *207*, 2232.
46. Hoffman, J.; Davis, G.; Lauritzen, Jr, J. In *Treatise on Solid-State Chemistry*; Hannay, N. B., Ed.; Plenum: New York, **1976**; Vol. 3.
47. Gan, Z.; Abe, H.; Doi, Y. *Biomacromolecules* **2001**, *2*, 313.
48. Williams, M.; Landel, R.; Ferry, J. *J. Am. Chem. Soc.* **1955**, *77*, 3701.
49. Ozawa, T. *Polymer* **1971**, *12*, 150.
50. Tobin, M. *J. Polym. Sci. Polym. Phys. Ed.* **1974**, *12*, 399.
51. Tobin, M. *J. Polym. Sci. Polym. Phys. Ed.* **1976**, *14*, 2253.
52. Tobin, M. *J. Polym. Sci. Polym. Phys. Ed.* **1977**, *15*, 2269.
53. Qiu, Z.; Zhou, H.; Mo, Z.; Zhang, H.; Wu, Z. *Polym. J.* **2000**, *32*, 287.